EFFECT OF WHEEL WEAR ON CONTACT LENGTH, UNCUT CHIP THICKNESS AND FORCES FOR A DEFORMABLE GRINDING WHEEL AND WORKPIECE

Andrew Warkentin and Robert Bauer
Department of Mechanical Engineering, Dalhousie University, 5269 Morris Street Room C360
Halifax, Nova Scotia, B3J 1B6
Corresponding author: Robert Bauer, robert.bauer@dal.ca

Received September 2006, Accepted October 2007
No. 06-CSME-45, E.I.C. Accession 2964

ABSTRACT

In this paper, contact length, uncut chip thickness, and contact forces were studied as the wheel wore during dry surface grinding of 4130 normalized steel for three different depths of cut (0.0025, 0.005, 0.0075 mm). An aluminum oxide grinding wheel (Norton 38A46HVBE) was used for all the experiments and the work and wheel speeds were 0.22 and 32.3 m/s, respectively. In each experiment, the wear flat area, the cutting edge density, the cutting edge width and length were determined using an automated optical measurement system. The grinding forces were measured using a force dynamometer. The contact length was determined using rigid-body, smooth-body and rough-body contact assumptions. The uncut chip thickness was determined using a continuity analysis. In this approach, the average volume of material is first determined by dividing the total material removal rate by the number of cutting edges. Then an assumption of the shape of the chip is made. In this work, the uncut chip was assumed to have a triangular profile and a rectangular cross-section. The uncut chip thickness can then be determined by dividing the average chip volume by the average contact length and chip width. In the experiments, grinding forces, wear flat area, cutting edge density increased and uncut chip thickness decreased as a result of wheel wear. In addition, the wheel wear increased the contact length significantly in the rough-body assumption, marginally in the smooth-body assumption but not in the rigid-body assumption. The normal contact pressure was determined by dividing the normal force by the product of the percent wear flat area and contact area. This result suggested that the rough body assumption represented the data most accurately.

LES EFFETS DE L'USURE DE LA MEULE SUR LA LONGUEUR DE CONTACT, L'ÉPAISSEUR DU COPEAU ET LES FORCES POUR UNE MEULE ET UNE PIÈCE DÉFORMABLE

RÉSUMÉ

Dans cet article, la longueur de contact, l'épaisseur du copeau et les forces de contact sont étudiés en tenant compte de l'usure de la meule pendant la rectification plane à sec d'acier 4130 pour trois profondeurs de coupe différentes (0.0025, 0.005, 0.0075 mm). Une meule en oxyde d'aluminium (Norton 38A46HVBE) est utilisée pour toutes les expériences et les vitesses de la pièce et de la meule sont respectivement de 0.22 et 32.3 m/s. Dans chaque expérience, l'usure de grains d'abrasifs, ainsi que la densité, la largeur et la longueur de l'arête tranchante sont déterminées en utilisant un système de mesure optique automatisé. Les forces présentes sont mesurées avec un dynamomètre. La longueur de contact est déterminée en utilisant différentes hypothèses de contact : corps rigide, corps lisse et corps rugueux. Une analyse de continuité est utilisée pour déterminer l'épaisseur de copeau. Selon cette approche, le volume moyen du matériau est d'abord déterminé en divisant le taux total d'enlèvement de matériau par le nombre d'arêtes tranchantes. Par la suite, une hypothèse sur la forme du copeau est faite. Dans ce travail, le copeau est présumé avoir un profil triangulaire et une section rectangulaire. L'épaisseur du copeau est par la suite déterminée en divisant le volume moyen du copeau par la longueur de contact moyenne et la largeur du copeau. Au cours des expériences, les forces de rectification, l'usure de grains d'abrasifs et la densité de l'arête tranchante augmentent tandis que l'épaisseur de copeau diminue avec l'usure de la meule. De plus, l'usure de la meule augmente la longueur de contact d'une façon importante dans l'hypothèse du corps rugueux, légèrement dans l'hypothèse du corps lisse mais pas du tout dans l'hypothèse du corps rigide. La pression normale est déterminée en divisant la force normale par le produit du pourcentage d'usure de grains d'abrasifs par la surface de contact. Ce résultat suggère que l'hypothèse du corps rugueux représente le plus adéquatement les données expérimentales.

INTRODUCTION

During grinding, the surface of the grinding wheel will wear causing changes in the grinding forces, the heat being generated and ultimately the quality of the ground surface. Researchers have recognized the existence of three distinct wear mechanisms in grinding: grain fracture, bond fracture, and attritious wear [1,2,3]. Small flat areas on abrasive grains called wear flats develop from attritious wear as abrasive grains rub against the workpiece. As the wear flat area increases, the sliding forces increase and more heat is generated, which eventually causes damage to the workpiece [1]. Therefore, the study of grinding wheel wear is important for the anticipation and prevention of wear-induced workpiece damage as well as the modeling and simulation of grinding forces. To date, grinding wheel wear studies have assumed that grinding wheels and workpieces are rigid bodies. However, it has been shown that the elastic deformation in the wheel-workpiece interface caused by grinding forces [4,5,6,7,8,9,10] has a significant effect on the contact mechanics of grinding. Specifically, the contact length between the wheel and workpiece is much greater than previously believed. Since the wheel wear affects the grinding forces it must also have an effect on the contact area. In this paper, the effect of wheel wear on the contact length, the uncut chip thickness and the contact forces will be examined, assuming three types of contact between the grinding wheel and the workpiece: rigid-body, smooth-body, and rough-body.

CONTACT LENGTH AND CHIP THICKNESS MODELS

In grinding, the contact length is the distance that an abrasive grit is in contact with the workpiece and the chip thickness is the maximum penetration of the abrasive grit into the workpiece. These parameters are fundamental to grinding mechanics but difficult to determine due to the stochastic nature of grinding wheel construction. The following section describes the models used to study the effect of wear on these parameters assuming rigid-body contact, smooth-body contact, and rough-body contact. More details on the derivations of the following relationships can be found in references [11] and [12].

Figure 1 shows the basic rigid-body cutting geometry for surface grinding typically used for determining the contact length and uncut chip thickness when the ratio of depth of cut to wheel diameter is small as in the surface grinding experiments conducted for this paper. More complex expressions exist for instances when the ratio of depth of cut to wheel diameter is larger as in creep-feed grinding with small wheels [12]. The grinding wheel has a diameter d_s, rotates at a surface velocity of v_s, and is fed into the workpiece at a velocity v_w. The distance that the wheel plunges into a workpiece is known as the depth of cut a. For simplicity, in Figure 1 only two adjacent cutting edges on the circumference of the wheel have been shown. These cutting edges are separated by a distance L along the circumference of the wheel. Each grain is assumed to follow a circular path. If the wheel and the workpiece are assumed to be rigid then the geometric contact length l_g is approximately [12]:

$$l_g = \sqrt{ad_s} \tag{1}$$

The maximum depth that the cutting edges penetrate into the workpiece is called the uncut chip thickness h_m and is typically expressed by [12]:

$$h_m = 2L\frac{v_w}{v_s}\sqrt{\frac{a}{d}} \tag{2}$$

As can be seen in Equation (2), the spacing between the cutting edges must be known in order to determine the uncut chip thickness. Figure 2(a) shows a rectangular patch on the grinding wheels surface of length L equal to the average grain spacing along the circumference of the grinding wheel, and a width B equal to the average grain spacing across the width of the grinding wheel. The average width and length of each of the cutting edges is b_c and w_c as shown in Figure 2(c). The cutting edges must be arranged such that the mean spacing between cutting edges equals the average cutting edge width in order for all the material to be removed from the workpiece if the cross-sections of the grains are assumed not to change with depth [11]. This concept is illustrated in Figure 2(b) by shifting the cutting edges so that they form a diagonal line. The cutting edge density C is equal to the number of cutting edges k divided by the total area [11].

$$C = \frac{k}{LB} \tag{3}$$

The grain spacing L can be determined by considering an area of width b_c that contains only one cutting edge [11]. Equation (3) then becomes:

$$C = \frac{1}{Lb_c} \tag{4}$$

Equation (4) can then be rearranged to solve for L as follows:

$$L = \frac{1}{Cb_c} \tag{5}$$

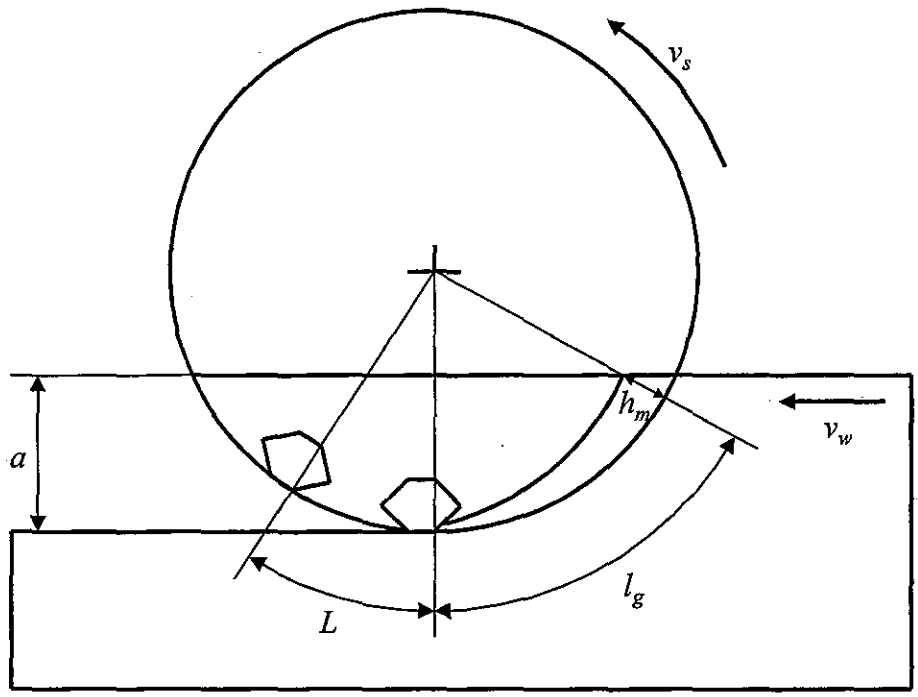

Figure 1: Cutting geometry in grinding.

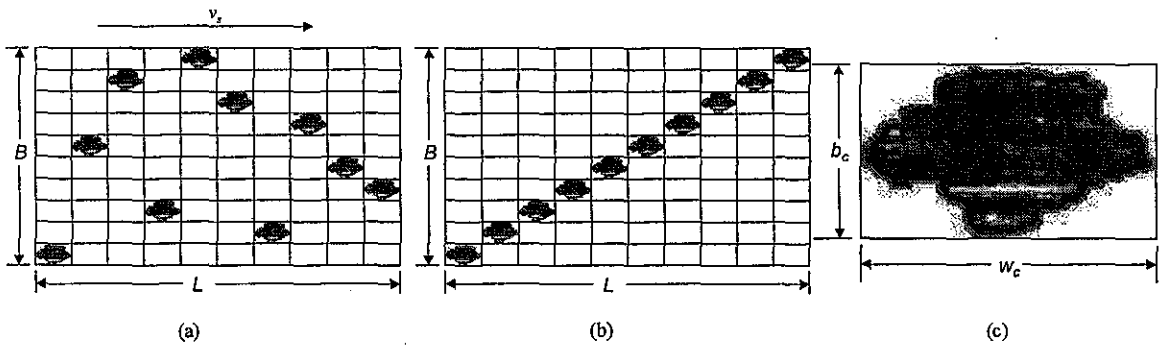

Figure 2: Cutting edge density and grain spacing.

The previous derivation of contact length assumed that the wheel and workpiece are rigid bodies. Several researchers have shown that the contact length is much longer due to the elastic nature of the grinding wheel and workpiece [4,5,6,7,8,9,10]. Rowe *et al.* [19] proposed that the contact length could be modeled using the following expression:

$$l_c = \sqrt{\frac{8R_r^2 F_n d_s}{\pi E^* b_w} + l_g^2} \qquad (6)$$

The second term under the square-root sign in Equation (6) is the contribution to the contact length due to the wheel workpiece geometry, while the first term is the contribution to the contact length due to elastic deformation. This elastic deformation term is based on the analysis of smooth spheres in contact developed by Hertz in 1882. The grinding wheel and the workpiece are assumed to be infinite cylinders and the contact pressure is assumed to have a parabolic distribution. F_n is the normal force, b_w is the width of the workpiece, and E^* is the combined elastic modulus of the workpiece and the wheel given by:

$$\frac{1}{E^*} = \frac{1 - \nu_1^2}{E_1} + \frac{1 - \nu_2^2}{E_2} \tag{7}$$

where ν_1, ν_2, E_1 and E_2 are Poisson's ratios and the modulus of elasticity for the two surfaces. The fact that the grinding wheel is not a smooth body is accounted for by using a roughness factor R_r which is the ratio of rough to smooth contact lengths. A value of $R=0$ corresponds to rigid-body contact, a value of $R=1$ corresponds to smooth-body contact, and a value of $R = 9$ has been found to be a reasonable value for rough-body contact in dry grinding [11].

Given the contact length, the uncut chip thickness can then be determined using the continuity analysis as described in [12]. In this analysis the material removal rate must equal the volume of chips produced by the cutting edges as shown in Equation (4),

$$\left(Cb_w v_s V_c\right) = a v_w b_w \tag{8}$$

where V_c is the chip volume. If the chip is assumed to have a rectangular chip cross section, then the chip volume is:

$$V_c = \frac{1}{2} h_m b_c l_c \tag{9}$$

Thus the uncut chip thickness can be determined by combining and rearranging Equations (8) and (9).

$$h_m = 2\left(\frac{1}{C}\right)\left(\frac{v_w}{v_s}\right)\left(\frac{a}{b_c l_c}\right) \tag{10}$$

Note that Equation (10) simplifies to Equation (2) if Equation (6) with $R_r = 0$ is substituted for l_c and Equation (5) is substituted for C.

EXPERIMENTAL APPARATUS

One of the most challenging aspects of this research was to experimentally determine the surface characteristics of the grinding wheel. Some of the methods employed by other researchers include imprint methods [13,14], profilometry [15], dynamometer and thermocouple techniques [16,17,4,18], and optical methods [19,20].

The Fully Automated Surface Condition Analysis Tool (FASCAT) developed by Lachance et. al. [21,22] was used to measure wear flat area and cutting edge density as shown in Figure 3. FASCAT captures images of the wheel surface with a Charge Coupled Device (CCD) digital camera. To achieve the maximum contrast between the wear flats and the background, the camera's viewing direction is in line with the light reflected from the wear flats, and perpendicular to the grinding wheel surface. During image acquisition, a feedback loop controlled by a PC is used to ensure that pre-programmed wheel positions are reached and captured by the camera. The positioning system can be programmed to acquire images from any number of positions on the wheel. Collecting 40 pictures, which represents approximately 10% of a 14" wheel circumference, requires less than 4 minutes. Image acquisition and positioning software for the new system was written in LabVIEW. To improve the performance of FASCAT, its original 8-bit, 640 × 480 pixel analog camera was upgraded to a 10-bit 1360×1024 pixel digital camera. Figure 4 shows a sample image of the surface of the wheel where the wear flats appear as bright areas. A region growing method described in [13] was used to identify the wear flats which have been outlined in white.

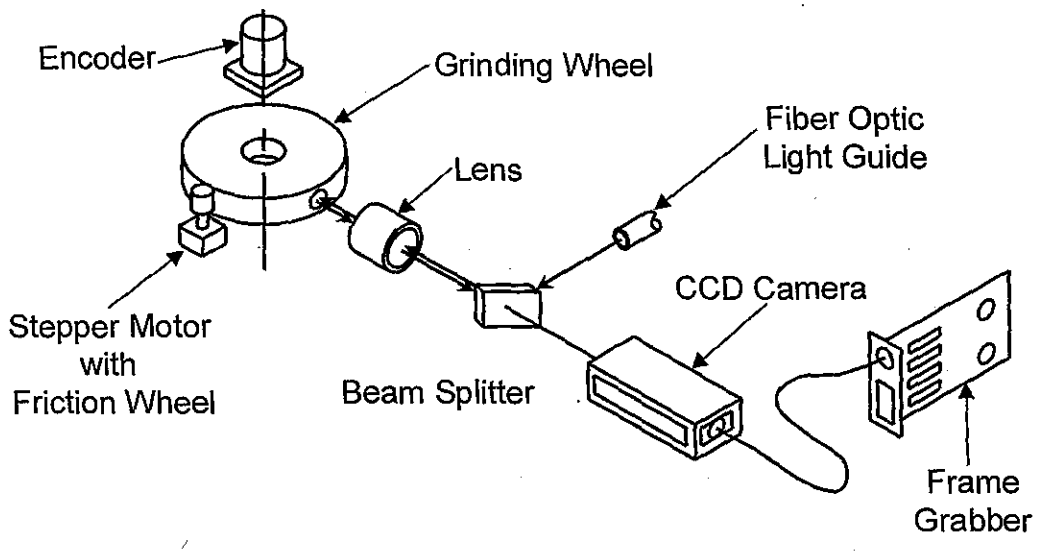

Figure 3: The FASCAT System [21].

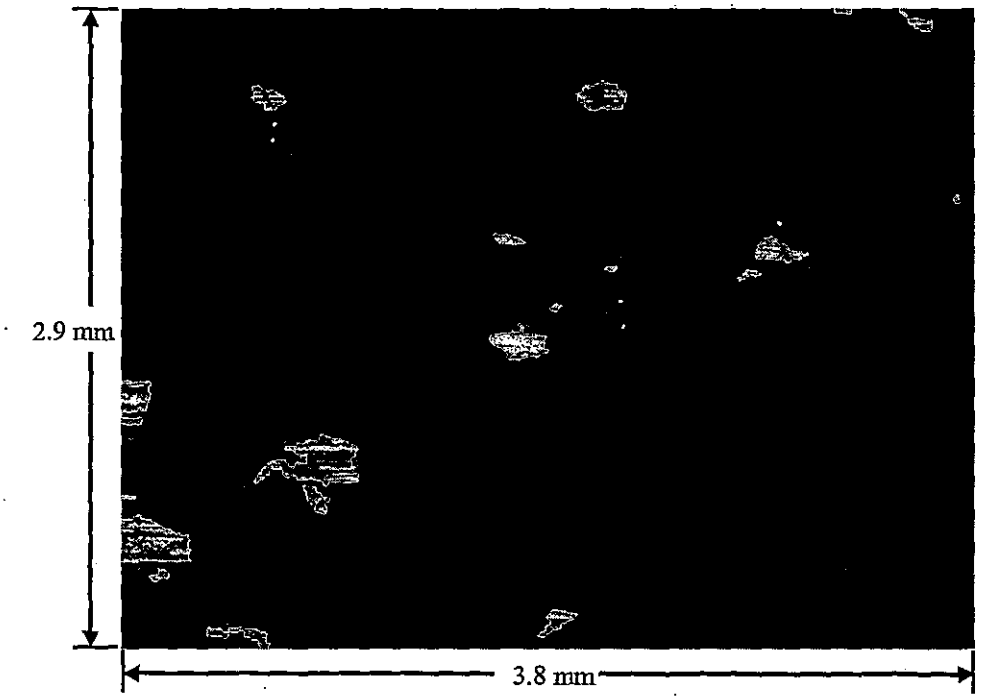

Figure 4: Sample image from FASCAT

Dry shallow grinding experiments were carried out on a Blohm Planomat 408 grinding machine using the process parameters shown in Table 1. Horizontal and vertical forces were measured with a Kistler 9257B Force Dynamometer and amplified with a Kistler 5019 Charge Amplifier. Spindle power was measured using a Load Controls Inc PH-3A Power Transducer. The modulus of the elasticity and Poisson's ratio for the grinding wheel was found to be 27.3 GPa and .27 using a Grindosonic instrument.

Table 1: Experimental parameters

Parameter	**Description**
Type of Dressing	Roll Dressing Dressing ratio of 1, 2 roll out passes
Grinding wheel	Norton 38A46HVBE
Workpiece material	4130 normalized steel
Workpiece dimensions (length× width× height)	152.4×6.1× 50.8 mm
Peripheral Velocity of Grinding Wheel	32.3 m/s
Grinding Wheel Diameter	353 mm
Feed rate of Workpiece	0.22 m/s

RESULTS AND ANALYSIS

Three sets of experiments were carried out for depths of cut of a=0.0025mm, a=0.005mm, and a=0.0075mm. The measured experimental data consists of the percent wear flat area (wear flat area/image area*100), the grain width, the cutting edge density, the normal and tangential forces. The measurements were taken approximately every 400 passes until workpiece burn was observed. Figures 5 and 6 plot these measurements as a function of the number of grinding passes. It can be seen from these figures that all of the measurements increase over time and the larger the depth of cut, the larger the measured values. These experimental results are consistent with the literature (see for example Malkin [12]). It appears that rubbing of the cutting edges on the workpiece causes a small amount of material removal from the grains resulting in the formation of wear flats in a process somewhat similar to the flank wear that occurs on conventional cutting tools. The removal of material from the grinding wheel allows more cutting edges to become engaged in grinding the workpiece which causes the cutting edge density to increase. At the same time grinding forces and power increase because the worn cutting edges are not as sharp.

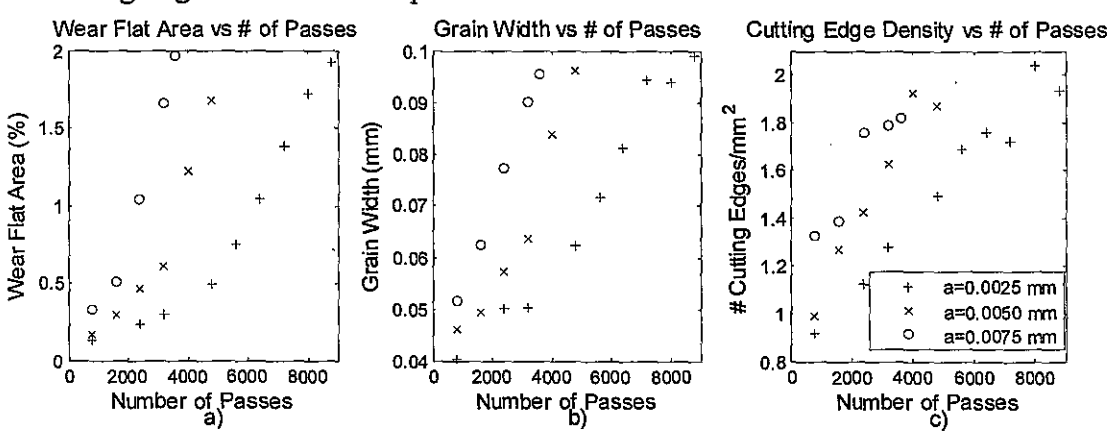

Figure 5: Wear flat area, grain width and cutting edge density as a function of number of passes.

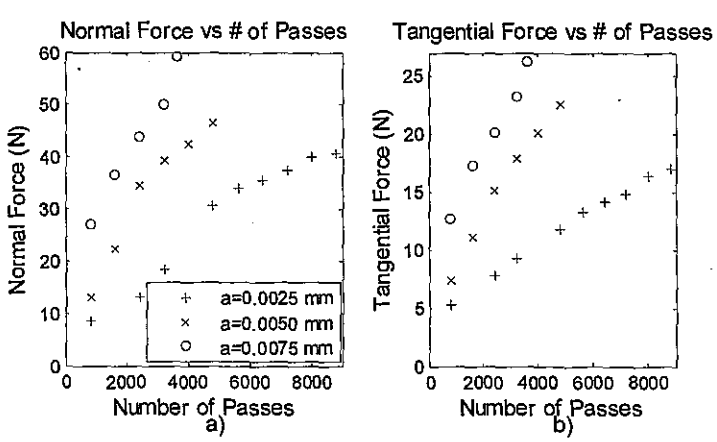

Figure 6: Normal and tangential force as a function of number of passes.

The grain contact area is the total wear flat area in the contact area and can be found from Equation (11):

$$A_a = b_w l_c \frac{A}{100} \tag{11}$$

where A is the percent wear flat area. Figure 7 plots the grain contact area as a function of number of passes for rigid ($R=0$), smooth ($R=1$) and rough ($R=9$) body contact. The results for the rigid body case ($R=0$) are typical; the grain contact area increases with the depth of cut and increases at approximately a linear rate with the number of passes indicating that the number and size of the wear flats is increasing over time. Compared to the rigid body case, the smooth body case shows a small increase in grain contact area as the number of passes increase, while the rough body case shows a significant increase in grain contact area with number of passes. The reason for this significant increase is because the increase in the normal force due to wheel wear increases the contact area through elastic deformation.

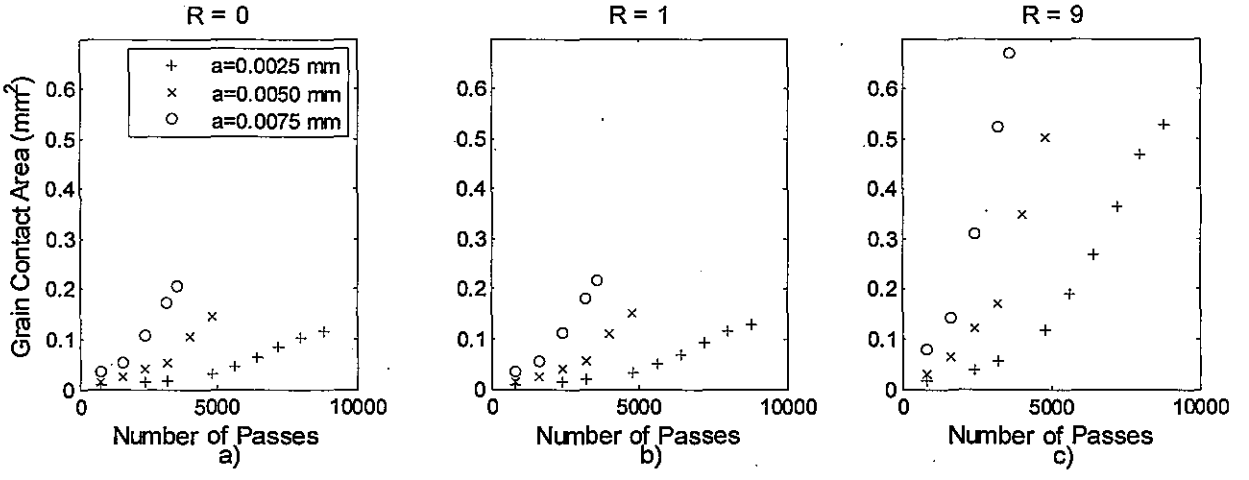

Figure 7: Grain contact area as a function of number of passes.

Figure 8 plots the normal and tangential forces as a function of the grain contact area for rigid ($R=0$), smooth ($R=1$) and rough ($R=9$) body contact. All the curves show that the forces initially increase rapidly as the wheel breaks in, and then increase at a more or less constant rate – which is consistent with most wear phenomena. Both the normal and tangential forces show a small increase due to the depth of cut; however, this increase is not as profound as can be observed in Figure 6 indicating that the depth of cut influences the forces less than grain contact area. The smooth and especially rough body contact cases show that forces are increasing less quickly than the rigid body case because the grinding forces are being spread over more asperities as the wheel wears.

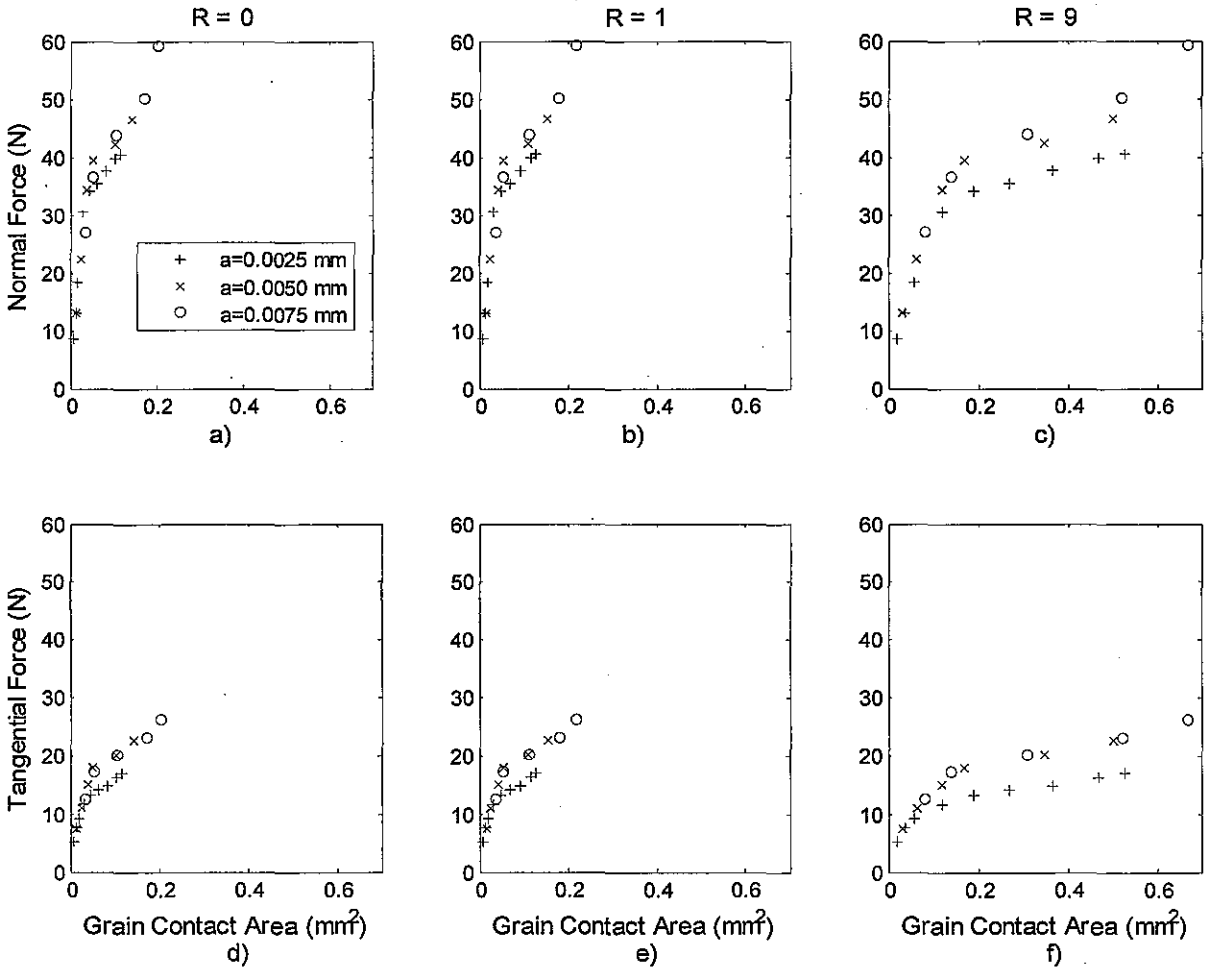

Figure 8: Normal and tangential force as a function of grain contact area for rigid, smooth and rough body contact.

Figure 9 shows the contact length and the maximum uncut chip thickness versus the grain contact area for different roughness factors R. For all values of R, both the contact length and the maximum uncut chip thickness increase with the depth of cut because more material is being removed from the workpiece. When $R=0$, the contact length is constant. As R increases, the contact length increases and the maximum uncut chip thickness decreases to account for the elastic deformation in the grinding zone and to maintain a constant chip volume. The effect of wear on the contact length and uncut chip thickness can be clearly seen for a roughness factor of 9. As the wheel wears, the contact area increases due to the increase in the wear flat area and the increase in normal force resulting in a significant increase in the contact length and decrease in the uncut chip thickness.

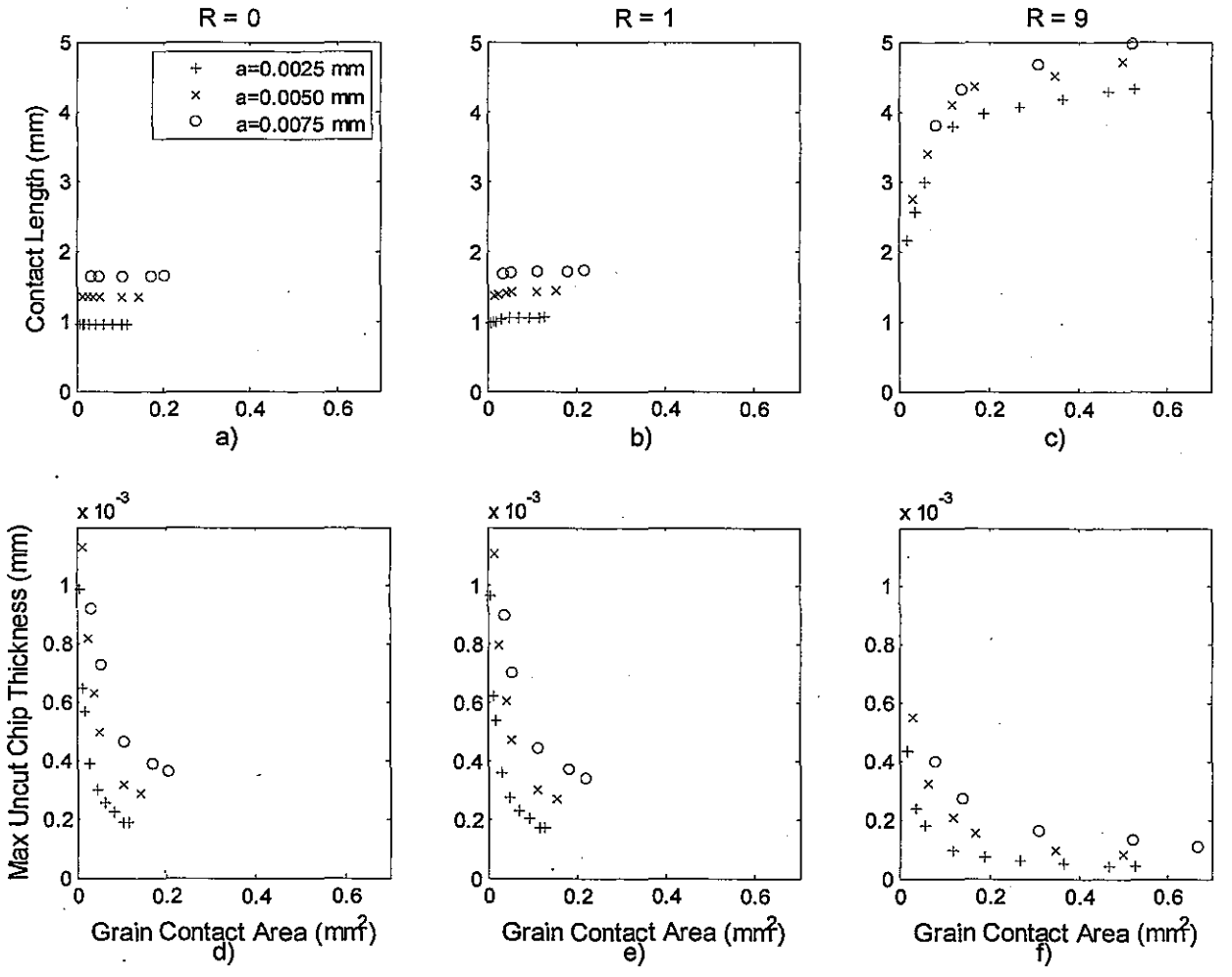

Figure 9: Contact length and uncut chip thickness as a function of grain contact area for rigid, smooth and rough body contact.

Table 2 summarizes the effect of wheel wear in the experiments for a depth of cut *a=0.0025*mm for roughness factors of *R=0, 1* and *9*. The normal force, tangential force, chip width, cutting edge density, percent wear flat area, and grain spacing are all measured quantities. The remaining quantities depend on the type of contact assumed. The contact length remained approximately constant when *R=0* and *R=1*, but increased by a factor of 2.0 when *R=9* due the increase in normal force. For *R=0* and *R=1*, the uncut chip thickness decreased by a factor of 5.2 and 5.6, respectively due to an increase in the cutting edge density. For *R=9*, the uncut chip thickness decreased by a factor of 10.5 due to an increase in both the contact length and cutting edge density. The grain contact area increased in all cases because it is the product of percent wear flat area and the contact area.

The contact pressure was also determined for each roughness factor and is summarized in Table 2. The contact pressures decreased in all cases as a result of wheel wear; however, the actual values were significantly larger when $R=0$ and $R=1$ than when $R=9$. Note that under the rigid body and smooth body assumptions, the contact pressure was greater than the ultimate tensile strength of the material (~650 MPa) which intuitively does not make sense because the workpiece must be able to support the wheel. This observation can be further justified using the theory proposed by Marinescu *et al.* [11] and illustrated in Figure 10. In this figure, the normal force is spread over a number of asperities in the contact zone. The contact length increases until enough asperities are in contact with the workpiece to support the normal force without exceeding the flow stress of the workpiece material. Based on this theory, the contact length on both the rigid body and smooth body cases is insufficient to support the grinding wheel in the newly dressed and worn conditions. Furthermore, the data suggests that the roughness factor may be less than 9 in the worn wheel condition, which would suggest that as the wheel wears it becomes smoother.

Table 2: Sample chip parameters, $a=.0025$mm

Wheel Condition	Newly Dressed	After 8800 Passes
Normal Force (N)	8.5	41
Tangential Force (N)	5.2	17
Chip width b_c (mm)	0.04	0.1
Cutting edge density C (# of cutting edges/mm^2)	0.91	1.9
Percent Wear Flat Area (%)	0.13	1.9
Grain spacing L (mm)	27	5.2
R=0:		
Contact length l_c (mm)	0.95	0.95
Maximum uncut chip thickness h_m (μm)	0.99	0.19
Grain contact area A_a (mm^2)	0.008	0.115
Normal Contact Pressure (MPa)	1090	352
R=1:		
Contact length l_c (mm)	0.97	1.06
Maximum uncut chip thickness h_m (μm)	0.96	0.171
Grain contact area A_a (mm^2)	0.008	0.129
Normal Contact Pressure (MPa)	1060	315
R=9:		
Contact length l_c (mm)	1.8	3.4
Maximum uncut chip thickness h_m (μm)	0.52	0.052
Grain contact area A_a (mm^2)	0.015	0.42
Normal Contact Pressure (MPa)	567	97.6

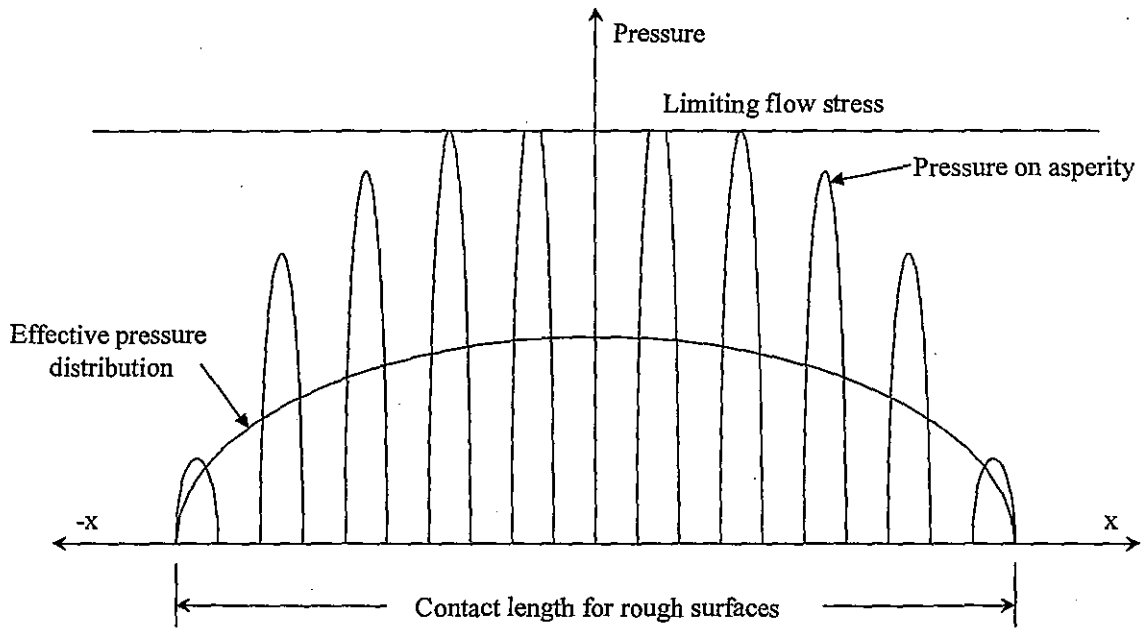

Figure 10: Pressure distribution for rough surfaces in contact [11]

CONCLUSIONS

A new automated optical method was used to measure the wear flat area, the grain length and width, and the cutting edge density – values which are traditionally challenging to measure. The contact length was determined using the assumptions of rigid-body, smooth-body and rough-body contact. The maximum uncut chip thickness was then found using a continuity equation with the assumption of a rectangular chip cross-section. To investigate the validity of the rough body assumption, the normal contact pressure was determined from the contact length, the wear flat area and the normal force.

It was found that wheel wear resulted in an increase in the normal and tangential grinding forces, as well as the wear flat area and the number of cutting edges. Under the assumption of rigid and smooth body contact, the wheel wear had a negligible influence on the contact length, while the uncut chip thickness decreased because the number of cutting edges increased. Under the assumption of a rough body contact, the wheel wear increased the contact length which further decreased the uncut chip thickness.

The normal contact pressures suggest that the rough body assumption is more reasonable because, in the rigid and smooth body assumptions, the contact pressures exceeded the ultimate strength of the material implying that the material could not support the grinding wheel. The normal contact pressure was also found to decrease due to wheel wear which also suggests that the wheel was getting smoother and that the roughness factor should likely be changed as the wheel wears.

ACKNOWLEDGMENTS

The authors would like to thank the Natural Sciences and Engineering Research Council of Canada (NSERC) and the Canadian Foundation for Innovation (CFI) who provided financial support for this work, and Sameer Khatri for his help in conducting the experiments.

REFERENCES

[1] S. Malkin and N.H Cook, The wear of grinding wheels. Part I, attritious wear, Journal of Engineering for Industry, Trans. ASME 93(4) (1971) 1120-1128

[2] S. Malkin and N.H. Cook, The wear of grinding wheels. Part II, fracture wear, Journal of Engineering for Industry, Trans. ASME 93(4) (1971) 1129-1133

[3] H. Yoshikawa and T. Sata, Study on wear of grinding wheels. Part 1. Bond fracture in grinding wheels, Journal of Engineering for Industry, Trans. ASME 85 (1963) 39-43

[4] J. Verkerk and A. J. Pekelharing, The real contact length in cylindrical plunge grinding, Annals of the CIRP 24(1) (1975) 259-265

[5] R. H. Brown, K. Sato, and M. C. Shaw, Local Elastic Deflections in Grinding, Annals of the CIRP 19(1) (1971) 105-113

[6] D. Y. Gu and J. G. Wager, New evidence on the contact zone in grinding - contact length, sliding and cutting regions Annals of the CIRP 37(1) (1988) 335-338

[7] Z. X. Zhou and C. A. Van Luttervelt, The real contact length between grinding wheel and workpiece. A new concept and a new measuring method, Annals of the CIRP 41(1) (1992) 387-391

[8] H. S. Qi, W. B. Rowe and B. Mills, Contact length in grinding. Part 1: Contact length measurement, Proceedings of the Institution of Mechanical Engineers, Part J: Journal of Engineering Tribology 211(1) (1997) 67-76

[9] H. S. Qi, W. B. Rowe and B. Mills, Contact length in grinding. Part 2: Evaluation of contact length models, Proceedings of the Institution of Mechanical Engineers, Part J: Journal of Engineering Tribology 211(1) (1997) 77-85

[10] W. B. Rowe, H. S. Qi, M. N. Morgan and H. W. Zheng, The real contact length in grinding based on depth of cut and contact deflections. Proceedings of the 13th International MATADOR Conference, Manchester (1993) 187-193

[11] I. D. Marinescu, W. B. Rowe, B. Dimitrov and I. Inasaki, Tribology of Abrasive Machining Processes, William Andrew Publishing. Norwich, New York, 2004

[12] S. Malkin, Grinding Technology: Theory and Applications of Machining with Abrasives, SME, Michigan, 1989

[13] W. R. Backer, E. R. Marshall and M. C. Shaw, The size effect in metal cutting, Transactions of ASME 74 (1952) 61-72

[14] K. Nakayama, Grinding wheel geometry, Proceedings of the International Grinding Conference, Pittsburgh (1972) 197-219

[15] S. M. Pandit and G. Sathyanarayan, A model for surface grinding based on abrasive geometry and elasticity, Journal of Engineering for Industry, Trans. ASME 104(4) (1982) 349-357

[16] J. N. Brecker and M. C. Shaw, Measurement of the effective number of cutting points in the surface of a grinding wheel, IEEE Conference Publication, Japan Society of Precision Engineering (1974) 740-745
[17] J. Peklenik, The statistical mechanism of chip formation in grinding process, IEEE Conference Publication, Japan Society of Precision Engineering (1974) 51-57
[18] L. Tigerstrom, Dynamic measuring of number of grinding edges and determination of chip parameter, SME Technical Paper (Series) MR, n MR79-40 (1979) 4p
[19] H. Tsuwa, Investigation of grinding wheel cutting edges, Journal of Engineering for Industry, Trans. ASME 86 (1964) 371-388
[20] T. Suto, T. Waida and T. Sata, In-process measurement of wheel surface in grinding operation, Proceedings of the Tenth International Machine Tool Design and Research Conference, (1969) 171-180
[21] S. LaChance, R. J. Bauer and A. Warkentin, Application of region growing method to evaluate the surface condition of grinding wheels, International Journal of Machine Tools & Manufacture 44(7-8) (2004) 823-829
[22] S. LaChance, A. Warkentin and R. J. Bauer, Development of an automated system for measuring grinding wheel wear flats, Journal of Manufacturing Systems 22(2) (2003) 130-135